

Dynamical diffraction effects in noninertial neutron interferometry

Ulrich Bonse

Institut für Physik, Universität Dortmund, 4600 Dortmund 50, Federal Republic of Germany

Thomas Wroblewski

*Institut Laue Langevin, Avenue des Martyrs, 156 X, 38042 Grenoble, France
and Institut für Physik, Universität Dortmund, 4600 Dortmund 50, Federal Republic of Germany*

(Received 30 January 1984)

Neutron interferometry performed in a noninertial frame is essentially influenced by dynamical diffraction effects occurring in the interferometer crystal which hitherto have not been taken into account. We have developed a corresponding theory from which a corrected phase shift is obtained which applies likewise to interferometry performed under the influence of gravity or on an accelerated neutron interferometer. The theory also predicts fading of interference contrast with increasing acceleration as was observed in the Colella-Overhauser-Werner gravity experiments but could not be explained unambiguously.

Interferometry with thermal neutrons^{1,2} is best accomplished with the single-crystal interferometer also used for x-ray interferometry.^{3,4} The principal layout of beams with such an instrument is shown in Fig. 1. Beams are split, recombined, and superimposed by Bragg diffraction occurring in crystal wafers *S*, *M_I*, *M_{II}*, and *A* which are all manufactured and remain coherent parts of a sufficiently large perfect single crystal of (usually) silicon. The phase shift β arising between interfering beams I and II may be calculated by evaluating the integral

$$\beta = \oint \vec{k}(\vec{r}) \cdot d\vec{r} \quad (1)$$

around the closed path formed by I and II. $\vec{k}(\vec{r})$ is the wave vector along this path. In the case of neutrons $\vec{k} = \vec{p}/\hbar$, where \vec{p} is the momentum to be determined from Schrödinger's equation

$$\left[-\frac{\hbar^2}{2m_i} \nabla^2 + V'(\vec{r}) \right] \Psi = E\Psi. \quad (2)$$

m_i is the inertial mass of the neutron. $V'(\vec{r})$ denotes the sum of all pertinent contributions to the potential, i.e., when applicable, those due to gravity ($-m_g \vec{g} \cdot \vec{r}$), to an acceleration \vec{a} of the frame of reference ($m_i \vec{a} \cdot \vec{r}$), to perfect crystal diffraction [$V_c(\vec{r})$: lattice periodic scattering potential of the crystal], etc.

Colella, Overhauser, and Werner⁵⁻⁸ (COW) have experimentally checked the validity of introducing gravity and reference-frame rotation into (1) in the manner described above. Measuring phase shifts on an interferometer which performed forced harmonic oscillations, we⁹ recently checked whether a potential $m_i \vec{a} \cdot \vec{r}$ allows correctly for an acceleration \vec{a} applied to the reference system.

Evaluating their experiment COW assume that Pendellösung effects which are typical for dynamical diffraction by a perfect crystal do not play a role in calculating the net phase shift due to gravity within the crystal medium.^{8,10} However, for the case of dynamical diffrac-

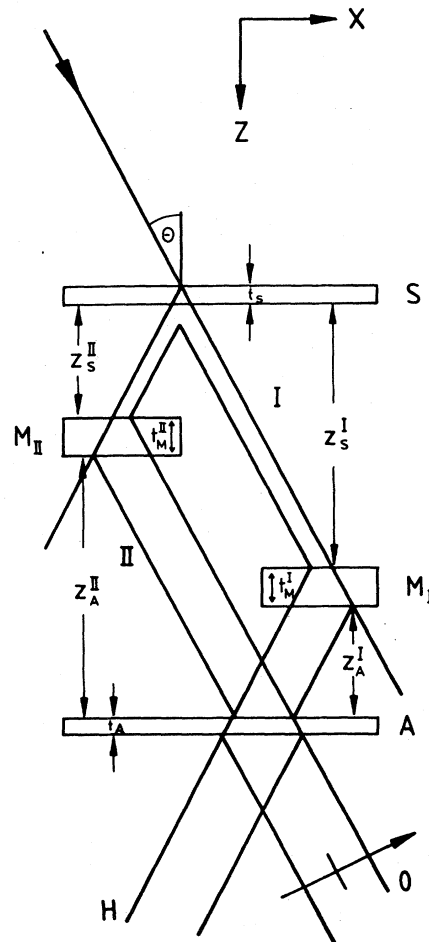


FIG. 1. Neutron interferometer consisting of splitter (*S*), mirrors (*M_I*, *M_{II}*), and analyzer (*A*) with thicknesses t_U ($U=S, M_I, M_{II}, A$) and distances Z_V^i ($V=S, A; i=I, II$). Via Bragg reflection the incoming neutron beam is split up into the beams I and II, which are reflected and recombined. The normal of the reflecting net planes is parallel to the *x* axis.

tion by just one crystal slab, Werner¹¹ has recently treated the influence of gravity on the dynamical diffraction process. Developing his approach further and applying it to the crystal sections S , M_I , M_{II} , and A of the interferometer of Fig. 1 when calculating the closed path integral (1) we obtain an essential correction to the gravity-induced phase shift. Furthermore, from our theory follows the fading of interference contrast observed in the COW experiment, which so far was unexpected and thus tentatively attributed⁸ to bending of the interferometer.

Introducing

$$V'(\vec{r}) = V_c(\vec{r}) + V(\vec{r}) \quad (3)$$

into (2) with $V(\vec{r}) \equiv -m_g \vec{g} \cdot \vec{r}$ in the case of gravity and $V(\vec{r}) \equiv m_i \vec{a} \cdot \vec{r}$ in the case of an accelerated frame, one gets¹¹ corrected dispersion surfaces with branches 1 and 2, on which, under the action of $V(\vec{r})$, the tie-points of wave fields travel in much the same way as they do in a uniformly bent crystal. Denoting p as the normalized local slope of the neutron trajectory, Werner derived for the change occurring over a traveling distance dz (Fig. 1)

$$\frac{d}{dz} [p(1-p)^{-1/2}] = \mp \tan \Theta_B \frac{2a_x m^2}{h^2 k_v^2 |\chi_l|}, \quad (4)$$

$$k_v \equiv \lambda_v^{-1},$$

where the upper sign stands for the branch-1 and the lower sign for the branch-2 wave field. χ_l is the Fourier component of order h_l of the normalized potential, $V_c(\vec{r})/E$. a_x is the component of the acceleration \vec{a} antiparallel to the reciprocal lattice vector \vec{h}_l . λ_v is the wavelength in vacuum.

Let, as usual, $\Delta\Theta \equiv \Theta - \Theta_B$ be the deviation from the exact Bragg angle Θ_B and y the corresponding deviation normalized to ± 1 at the limits of the dynamical reflection range. Then

$$\Delta\Theta = -y \frac{|\chi_l|}{\sin 2\Theta_B} = \pm p(1-p)^{-1/2} \frac{|\chi_l|}{\sin 2\Theta_B} \quad (5)$$

so that using Eqs. (4) and (5),

$$dy = \tan \Theta_B \frac{2a_x m^2}{h^2 k_v^2 |\chi_l|} dz. \quad (6)$$

It can be shown that (6) also holds outside the crystal. When the neutron enters the parallel-sided crystal wafers the wave vectors change accordingly:¹²

$$k_v \delta_{1,2} \equiv (\vec{K}_0^i - \vec{K}_{0,2}^i) \cdot \hat{z} = \frac{1}{2\Delta_0} \left[\frac{|\chi_0|}{|\chi_l|} + y \pm (y^2 + 1)^{1/2} \right], \quad (7)$$

$$k_v \delta'_{1,2} \equiv (\vec{K}_h^i - \vec{K}_{h,2}^i) \cdot \hat{z} = \frac{1}{2\Delta_0} \left[\frac{|\chi_0|}{|\chi_l|} - y \pm (y^2 + 1)^{1/2} \right], \quad (8)$$

$$k_v \delta \equiv (\vec{K}_{h,2} - \vec{K}_{0,2}^i) \cdot \hat{z} = -y / \Delta_0, \quad (9)$$

Δ_0 is the dynamical extinction length.

The upper index i denotes outside wave vectors. Lower indices o , h denote the wave vector traveling in the o , h direction (Fig. 1). Index 1 (2) and the upper (lower) sign are valid for the branch-1 (2) wave field, respectively.

When evaluating the integral of Eq. (1), the variation of y with z ,

$$y(z) = y_0 + \tan \Theta_B \frac{2a_x m^2}{h^2 k_v^2 |\chi_l|} z \equiv y_0 + bz, \quad (10)$$

has to be accounted for. For the path sections within the crystals, the phases of the transition factors¹² $\langle i | \alpha_U | j \rangle$ connecting the amplitudes in front of and behind a particular crystal wafer α [$\alpha = S, M_I, M_{II}, A$ (Fig. 1)] when the wave is diffracted from the i direction to j direction ($i=0, H; j=0, H$) via the wave field on branch U ($U=1, 2$) are obtained by integrating the expressions (7) to (9) along z . Terms originally linear in y give

$$\int_{z_i}^{z_f} (y_0 + bz) dz = y_0(z_f - z_i) + \frac{b}{2}(z_f^2 - z_i^2). \quad (11)$$

On the other hand, root terms give¹³

$$\int_{z_i}^{z_f} [(y_0 + bz)^2 + 1]^{1/2} dz = \frac{1}{2b} \left[y_f(y_f^2 + 1)^{1/2} - y_i(y_i^2 + 1)^{1/2} + \ln \frac{(y_f^2 + 1)^{1/2} + y_f}{(y_i^2 + 1)^{1/2} + y_i} \right]. \quad (12)$$

Subscripts i (f) denote the entrance (exit surface) of the wafer, respectively. Not only the phase factors are influenced by the acting acceleration but also the modules of wave amplitudes. Their modification is calculated by postulating particle conservation separately for either branch of the dispersion surface. For the complete interfering beam paths I and II (Fig. 1) we obtain transition factors

$$\begin{aligned} \langle 0 | I | 0 \rangle &= \sum_{U=1,2} \langle 0 | S_U | 0 \rangle \\ &\times \sum_{U=1,2} \langle 0 | M_{IU} | H \rangle \sum_{U=1,2} \langle H | A_U | 0 \rangle, \end{aligned} \quad (13)$$

$$\begin{aligned} \langle 0 | II | 0 \rangle &= \sum_{U=1,2} \langle 0 | S_U | H \rangle \\ &\times \sum_{U=1,2} \langle H | M_{IU} | 0 \rangle \sum_{U=1,2} \langle 0 | A_U | 0 \rangle. \end{aligned} \quad (14)$$

The terms of Eq. (11) give, with ideal geometries (i.e., $Z_S^I = Z_A^{II} \equiv Z_S$, $Z_A^I = Z_S^{II} \equiv Z_A$, $t_S = t_A$) a phase difference between beams I and II of

$$\beta_0 = \pi \frac{b}{\Delta_0} (t_M Z_S + t_M Z_A + 2Z_S Z_A), \quad (15)$$

which apparently is independent of y . This part was also calculated by Greenberger and Overhauser.¹⁰ However,

TABLE I. Oscillation frequencies q for six wavelengths λ between 0.1060 and 0.1831 nm for the COW interferometer. q_{exp} as measured and q_{COW} theoretical value by COW; c_{COW} bending correction according to COW, q_{dyn} : result of dynamical treatment given in this paper.

λ (nm)	q_{exp}	q_{COW}	$q_{\text{COW}} + c_{\text{COW}}$	q_{dyn}
0.1060	32.98	30.50	32.98	32.14
0.1136	37.85	35.26	37.92	37.10
0.1232	44.87	41.77	44.66	43.77
0.1419	60.30	56.41	59.73	58.79
0.1628	80.74	75.92	79.73	78.74
0.1831	103.27	98.98	103.27	101.89

an additional phase shift β_d is given through expression (12) and its evaluation shows that the dependence on y does not drop out of the equations. Since usually the beam divergence is larger than the dynamical acceptance range of the interferometer crystal one has to use spherical waves which implies integration with respect to y . Following the treatment by Bauspiess, Bonse, and Graeff,¹² we calculated interferograms for the COW interferometer ($Z_S = Z_A = 34.518$ mm, $t_S = t_M = t_A = 2.464$ mm) and the six wavelengths used in the COW experiment.⁸ The results, obtained with a , the acceleration normal to the Bragg planes ranging from -6.5 m sec⁻² to $+6.5$ m sec⁻², are summarized in Table I. By Fourier transforming the calculated interferograms we determined q_{dyn} which should be compared with $q_{\text{exp}} \equiv \beta_{\text{COW}}/\sin\phi$, the corresponding value measured and q_{COW} , the value calculated by COW. β_{COW} is the measured phase shift and ϕ the angle by which the interferometer was rotated about the incident beam. COW attributed the difference between q_{exp} and q_{COW} to bending (or warping) of the interferometer under its own weight with the elevation angle ϕ . From two interference measurements performed with Mo K_α x-rays and the 220 and 440 reflections, respectively, COW concluded a dependence of $q_{\text{exp}} - q_{\text{COW}}$ on λ proportional to λ^2 and consequently added the correction $c_{\text{COW}} \sim \lambda^2$ to q_{COW} . The reason for such a variation with λ could not be found. It appears unlikely that a simple change of path length¹⁴ is the cause for the observed discrepancy since a deformation of this amount would

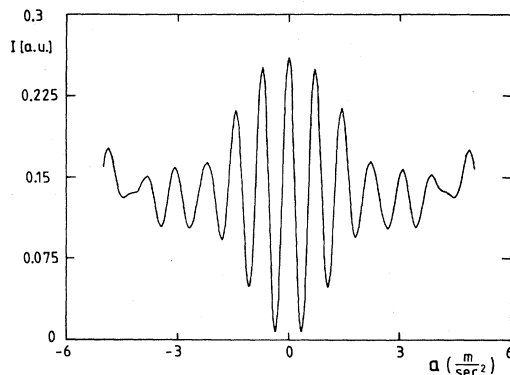


FIG. 2. Calculated intensity as a function of the acceleration in the x direction for the $D18$ interferometer at $\lambda=0.1839$ nm (ideal geometry assumed).

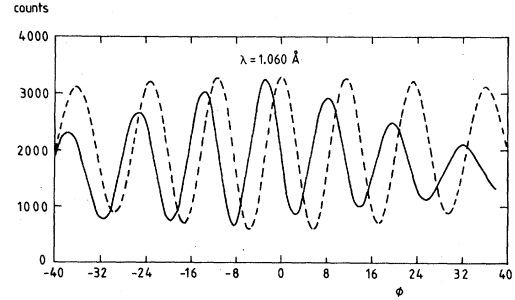


FIG. 3. Intensity as a function of the rotation ϕ (in degrees) around the incoming beam for the COW interferometer at $\lambda=0.1060$ nm. Full line: Values measured by COW.¹⁴ Broken line: Dynamical theory, contrast adapted to the maximum experimental value. (The theoretical contrast is 1 for ideal geometry and $a=0$. The curve is symmetric around $a=0$ because only linear acceleration was taken into account.) Note contrast fading also in the theoretical curve.

certainly cause even larger phase differences, e.g., by the rotational moiré effect¹⁵ or within the crystal wafers themselves through deformation-induced tie-point migration.

We also calculated an interferogram at $\lambda=0.1839$ nm for our interferometer crystal used with $D18$ at Grenoble ($Z_S = Z_A \equiv Z_W = 27.2936$ mm, $t_S = t_M = t_A \equiv t = 4.3954$ mm) (see Fig. 2). Because of the large ratio t/Z_W as compared to that of the interferometer crystal used by COW the discrepancy of the semiclassical theory (i.e., neglecting dynamical phase effects) with the experiments is larger. According to that theory $q=68.28$ rad, whereas by Fourier transformation of the interferogram of Fig. 2 we get $q=70.73$ rad. Furthermore, from Fig. 2 we see that with larger effective accelerations a the phase shift no longer varies linearly with a . From the position of the first minimum we find for small a $q=76.35$ rad. This value is confirmed by a recent experiment⁹ in which the interferometer crystal at Grenoble was subjected to defined accelerations. The prediction of the semiclassical theory is significantly different from the result of that measurement.

Furthermore, the dynamical theory predicts the fading of contrast at high accelerations in good agreement with the measurements of COW as can be seen in Figs. 3 and 4 (full line: COW experiment, broken line: dynamical theory, contrast adapted to its experimental value). The cause of fading can be explained by Eqs. (13) and (14). For simplicity we consider a symmetric interferometer ($Z_S = Z_A$). Because the transition factors depend on t , y ,

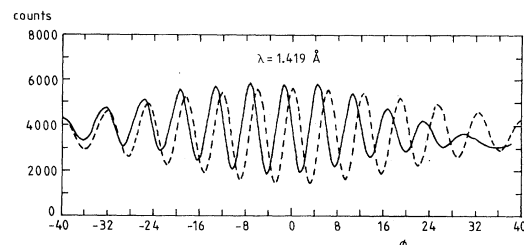


FIG. 4. Same as Fig. 3 except for $\lambda=0.1419$ nm.

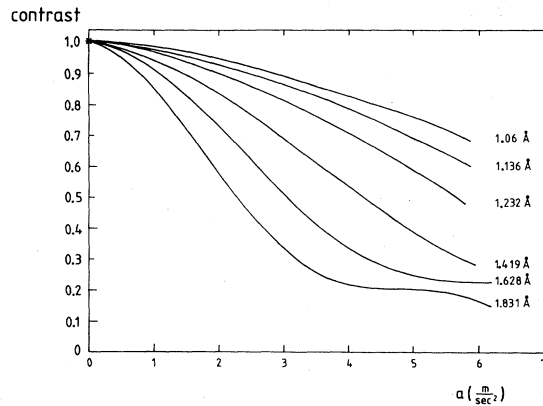


FIG. 5. Theoretical contrast as a function of acceleration for the six wavelengths used in the COW experiment (ideal geometry assumed).

and Δ_0 , for the transition factors of the two interfering beams, to remain equal it is not only necessary that splitter and analyzer have equal thickness¹² but also that y remains constant over the whole interferometer which, according to Eq. (10), is no more the case in a noninertial frame. Since the y dependence is weighted by

$$\frac{t}{\Delta_0} = \text{const} \frac{t\lambda}{(4d^2 - \lambda^2)^{1/2}}$$

(d = distance of the reflecting net planes) the fading effect should increase with t and λ . Indeed, the calculated contrast as a function of acceleration as well as the measurements of COW show this λ dependence (Figs. 3–5). The contrast as function of the acceleration-induced phase shift is shown in Fig. 6. It is independent of λ , for phase shift and contrast depend in the same way on t/Δ_0 . However, it depends on the ratio t/Z_W of wafer thickness to distance as can be seen from the curve calculated for the *D18* interferometer (Fig. 6). The ratio t/Z_W of the *D18* interferometer is $\frac{16}{7}$ times that of the COW interferometer

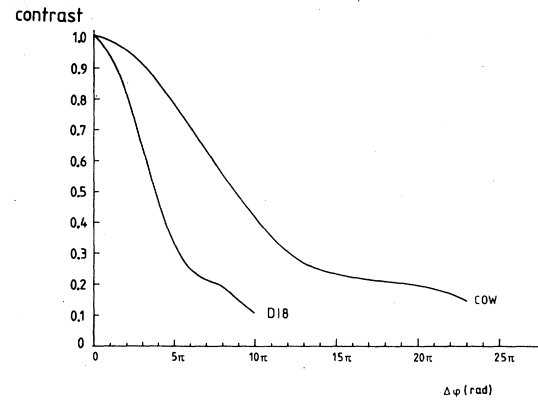


FIG. 6. Calculated contrast as a function of the acceleration-induced phase shift for the COW and the *D18* interferometer (ideal geometry assumed). The *D18* curve stretched by the factor $(t/Z_W)_{D18} (t/Z_W)_{COW}^{-1}$ coincides with the COW curve.

and so the *D18* curve stretched by this factor coincides with the COW curve.

It has been shown that dynamical diffraction theory is essential in describing neutron interferometry in noninertial frames, for it not only explains the acceleration-(gravity-) induced phase shift but also the fading of contrast. First hints on the incompleteness of the semiclassical COW theory were given by the COW experiment. Finally, an experiment with an accelerated interferometer⁹ confirmed the dynamical theory while the predictions of the semiclassical theory failed. The dynamical theory and the latter experiment not only showed in connection with the COW experiment the equivalence of inertial and gravitational mass, but also demonstrated that in quantum mechanics the peculiarities of the apparatus, i.e., the dynamical diffracting interferometer crystal, has to be taken into account.

We thank the Bundesminister für Forschung und Technologie, Bonn (03B56A01) for financial support.

¹H. Rauch, W. Treimer, and U. Bonse, Phys. Lett. **47A**, 369 (1974).

²*Neutron Interferometry*, edited by U. Bonse and H. Rauch (Clarendon, Oxford, 1979).

³U. Bonse and M. Hart, Appl. Phys. Lett. **6**, 155 (1965).

⁴U. Bonse and W. Graeff, in *X-Ray Optics, Topics in Applied Physics*, edited by H.-J. Queisser (Springer, Berlin, 1977), Vol. 22, p. 93.

⁵A. W. Overhauser and R. Colella, Phys. Rev. Lett. **33**, 1237 (1974).

⁶R. Colella, A. W. Overhauser, and S. A. Werner, Phys. Rev. Lett. **34**, 1472 (1975).

⁷S. A. Werner, J.-L. Staudenmann, and R. Colella, Phys. Rev. Lett. **42**, 1103 (1979).

⁸J. L. Staudenmann, S. A. Werner, R. Colella, and A. W. Overhauser, Phys. Rev. A **21**, 1419 (1980).

⁹U. Bonse, and T. Wroblewski, Phys. Rev. Lett. **51**, 1401 (1983).

¹⁰D. M. Greenberger and A. W. Overhauser, Rev. Mod. Phys. **51**, 43 (1979).

¹¹S. A. Werner, Phys. Rev. B **21**, 1774 (1980).

¹²W. Bauspiess, U. Bonse, and W. Graeff, J. Appl. Cryst. **9**, 68 (1976).

¹³I. N. Bronstein, and K. A. Semendjajew, *Taschenbuch der Mathematik* (Deutsch, Zürich and Frankfurt am Main, 1974).

¹⁴S. A. Werner, J. L. Staudenmann, R. Colella, and A. W. Overhauser, Ref. 2, p. 209.

¹⁵U. Bonse and M. Hart, Z. Phys. **190**, 455 (1966).